



INSA de Lyon & Kungliga Tekniska högskolan

Master of science in acoustics

Master thesis - Projet de fin d'étude

Measurements of liners acoustic properties

Francois DAYET
June 2017

KTH responsible:
Hans BODÉN
INSA responsible:
Etienne PARIZET

Acknowledgements

I'm grateful for the Marcus Wallenberg Laboratory for Sound and Vibration. It was a pleasure to work in this laboratory and use their facilities. It was for me a great opportunity to work in this acoustic environment.

I also want to show my gratitude to Luck Peerlings who helped me a lot. Thank you for your time and you very clear explanations.

I want to specially thank my supervisor Hans Bodén. The subject he proposed was very interesting and stimulating. I learn a lot of acoustic knowledge thanks to him. He gave me the opportunity to do high valued measurements with a rare setup.

I thank my co-workers and all the people with I spent a great time.

Contents

1	Introduction	2
2	Theoretical acoustic	4
2.1	Acoustic in duct	4
2.1.1	Rectangular duct	5
2.1.2	Circular duct	6
2.1.3	Wall attenuation	7
2.2	Scattering matrix	7
2.3	Impedance acoustic	8
2.3.1	Impedance tube measurement	8
2.3.2	The in-situ method	9
2.3.3	The mode matching method	10
2.3.4	The single mode straightforward method	12
2.4	Optimum Cremer impedance	13
2.4.1	Optimization of a circular liner	14
2.4.2	Optimization of an annular liner	15
3	Measurement and post-treatment	17
3.1	Experimental work	17
3.1.1	KTH facilities	17
3.1.2	The rig setup	18
3.1.3	Acquisition chain	20
3.1.4	Frequency domain and scattering matrix	21
3.2	Reference: hard wall case	22
3.3	Acoustic liner	23
3.3.1	Scattering matrix and transmission loss	23
3.3.2	Acoustic impedance	26
4	Conclusion	27
5	Appendix	29

1 Introduction

The noise pollution is one of the main issue of the XXIst century. It causes usual annoyances but it also threat health. The European Union highlights the risks of noise pollution [1]. The transports cause the highest noise pollution. A considerable effort has been made to reduce the emissions and continue to be made.

In the aircraft field, the noise has to be reduced inside the structure in order to keep a relative comfort for the passengers and also outside in the case because aircraft fly over habitations. The main source of noise in the aircraft is the engines.

The emission of noise in an engine is complex and due to different phenomenon. Nowadays, the usual engines type is by-pass turbofan engine. At the input of the duct, there is the admission of low pressure air. A fan pushes the air into the higher levels, the interaction between this fan and the stator is one of the principal source of noise. Thus, a high air ratio passes through the by-pass duct. The second path is the principal duct. The combustion is also a high source of emission. The air ejection is called a jet flow. The interaction between the ejected air flows with different velocities is a source of noise. The following figure shows the different sources of noise in a by-pass turbofan engine.

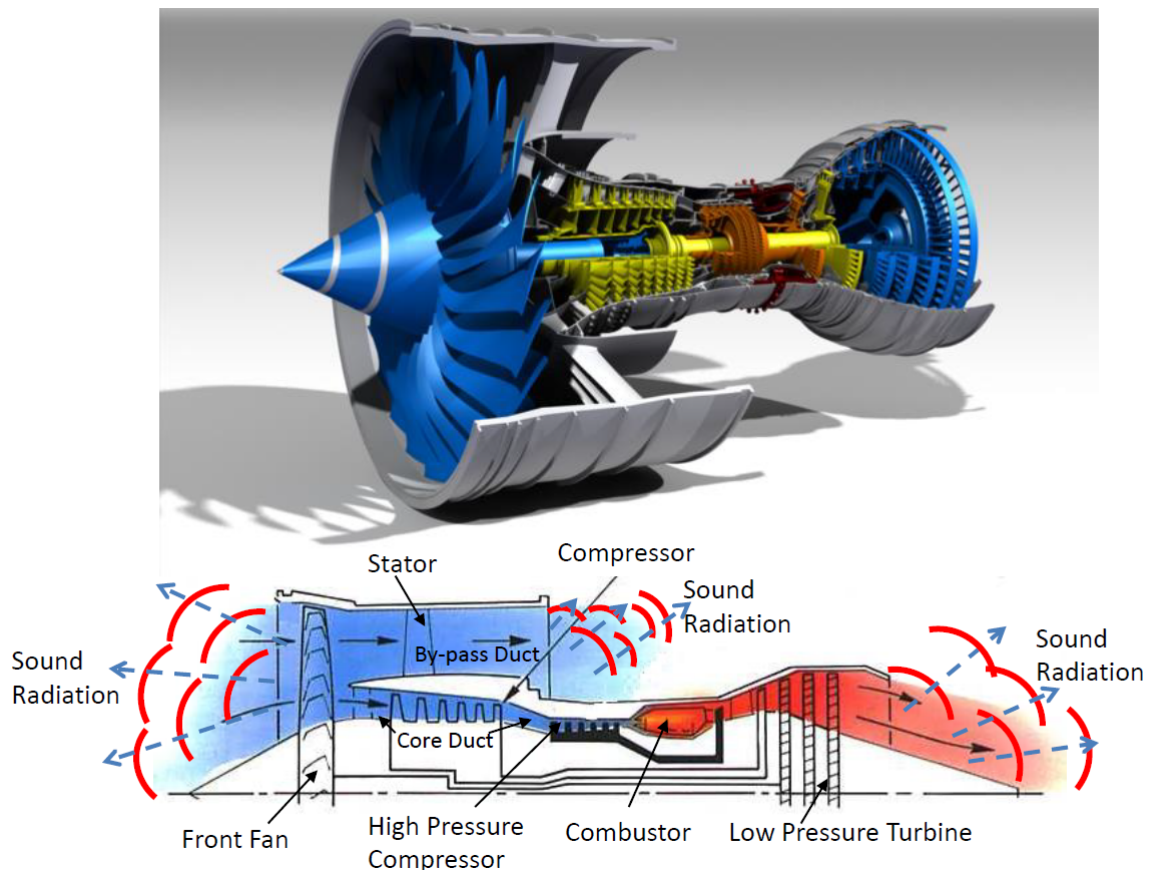


Figure 1: Different acoustic sources in engines [2]

To reduce the noise transmission, a liner acoustic is added in the engines walls. It is a perforated panel which contained a honeycomb structure. The small cavities can be compared to small Helmholtz resonators. The air in the orifices plays the role of mass and the cavity formed by the honeycomb structures acts as a spring.

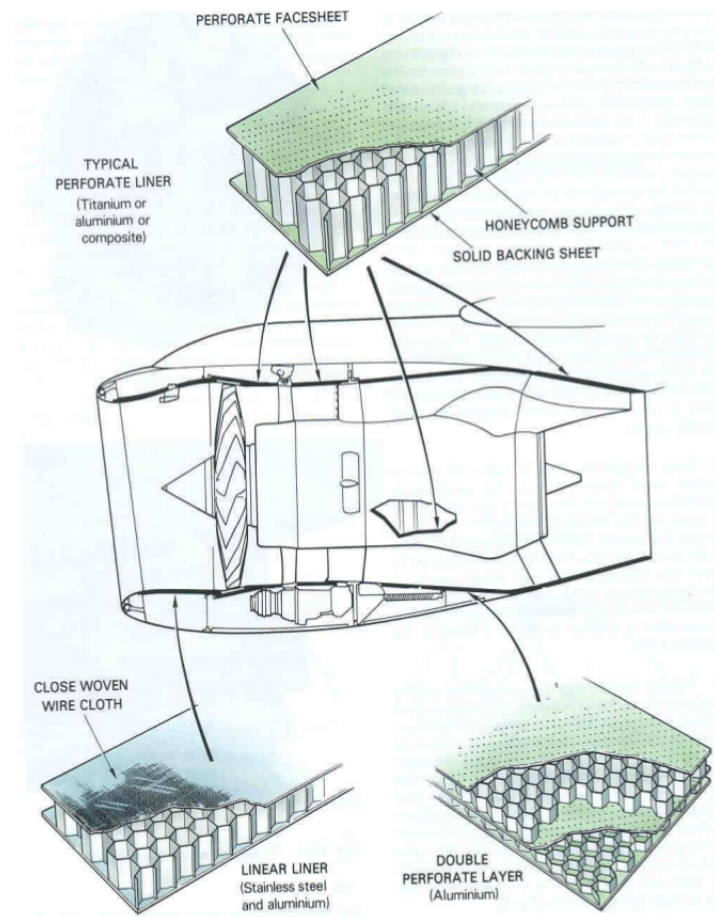


Figure 2: Typical perforate liner [3]

Aircraft suppliers need to well understand how work these liners to optimize the geometry or to add some porous material inside the honeycomb structures. However the problem is very difficult. Indeed the size of the acoustic waves in the engines are larger than the size of the hole ($\sim 0.5\text{mm}$). That's why it's very difficult to implement a finite-elements method. Some models are to be found to reduce this difficulty. The usual solution is to used the acoustic impedance of the liner:

- First, the wall impedance is find with the acoustic theory applied to small cavities.
- The impedance of the liner is used in a macro model.

This master thesis is part of the IMAGE project (Innovative Methodologies and technologies for reducing Aircraft noise Generation and Emission) which is in collaboration with European and Chinese laboratories.

2 Theoretical acoustic

2.1 Acoustic in duct

The acoustic in ducts is well-known and the main aspects were find by Helmholtz. A good overview can be found in this book [4]. We consider an infinite duct with x axis and a given section.

Acoustics is governed by few equations:

- Mass continuity:

$$\frac{\partial \rho}{\partial t} + \operatorname{div} \rho v = 0 \quad (1)$$

With ρ the density, v the velocity.

- Momentum continuity (given by the Navier-Stockes equation):

$$\rho \frac{dv}{dt} = -\operatorname{grad} \rho + \operatorname{div} \tau + g \quad (2)$$

- energy continuity

However, these equations are too complex to be used analytically. Some assumptions are made:

- Non-viscous fluid
- No thermal conductivity
- Entropy conservation
- Uniform mean flow
- Time dependence of $\exp(iwt)$. The section is constant across the x axis. Thus $p \propto \exp(iwt \pm ikx)$

With the mass continuity and the momentum continuity, the convective Helmholtz equation can be found:

$$\Delta p + \left[(w - ku_0)^2 - k^2 c_0^2 \right] p = 0 \quad (3)$$

With Δ the Laplace operator and c the sound speed velocity.

The solution of this equations is a sum of different functions called modes:

$$p(x, y, z, \omega) = \sum_{l=0}^{\infty} p_l^+ \Psi_l(y, z) e^{-ik_{x,l}(M,\omega)x} + p_l^- \Psi_l(y, z) e^{-ik_{x,l}(-M,\omega)x} \quad (4)$$

With M the mach number $M = v/c$. The l modes are sorted by frequency. Each mode has an acoustic shape in the section (y, z) . The mode can propagate in two different directions, in the positive or the negative direction. The usual problem in acoustic is the significant number of modes which are not negligible. In the duct, only few modes propagate unattenuated. Indeed, over a certain cut-off frequency $Re(k_{x,l})$ is negative, these modes are attenuated quickly. This cut-off frequency depends of the geometry and the mach number. For usual duct, just one mode propagates energy, the plane wave mode.

2.1.1 Rectangular duct

To solve Eq.(4), the separation of variables method is used. The mode shapes are independent between the directions y and z (called m modes for y direction and n for z). For rigid wall boundary conditions:

$$\Psi_{m,n}(y, z) = \Psi_m(y)\Psi_n(z) = \cos\left(\frac{m\pi y}{2b}\right)\cos\left(\frac{n\pi z}{2h}\right) \quad (5)$$

With b and h the width and the height. The axial wave number $k_{x,(m,n)}$ is solution of the dispersion equation:

$$k_{x,(m,n)} = k_0 \frac{M \pm \sqrt{1 - (1 - M^2) \left[\left(\frac{m\pi}{2ka} \right)^2 + \left(\frac{n\pi}{2kh} \right)^2 \right]}}{1 - M^2} \quad (6)$$

Mode will propagate if:

$$k \geq \sqrt{(1 - M^2) \left[\left(\frac{m\pi}{2a} \right)^2 + \left(\frac{n\pi}{2h} \right)^2 \right]} \quad (7)$$

The transverses waves numbers respect:

$$k_{y,(m)} = \frac{m\pi}{2a} \text{ and } k_{z,(n)} = \frac{n\pi}{2h} \quad (8)$$

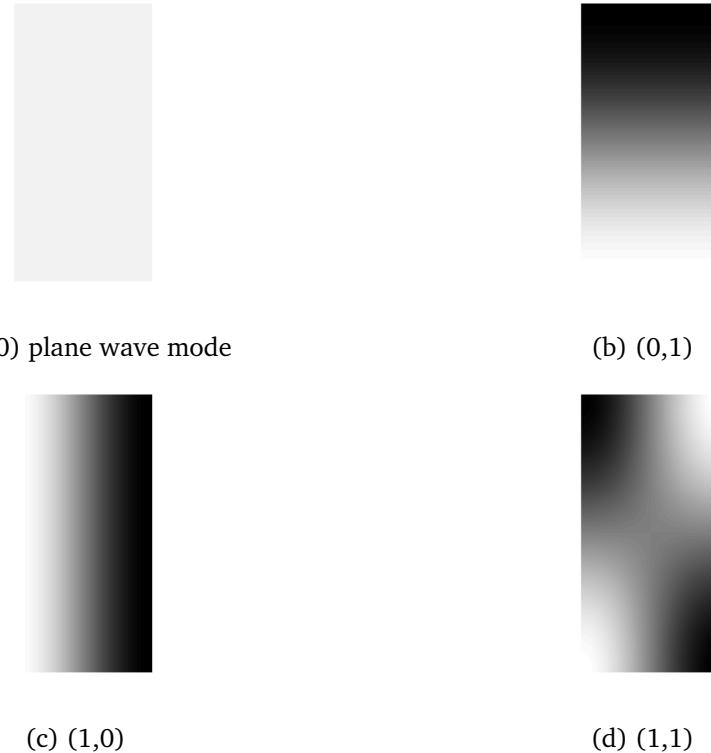


Figure 3: Mode shape (m,n) in a rectangular duct

2.1.2 Circular duct

The radius is called R ($0 < r < R$). For circular duct, there are two kinds of modes: **circumferential and radial modes (called respectively m and n)**. The mode shape is not independent between the radial and circumferential direction.

$$\Psi_{m,n}(r, \theta) = J_m(k_{r,(m,n)}r)e^{jm\theta} \quad (9)$$

Where $k_{r,(m,n)} = \frac{j_{mn}}{R}$. J_m is the Bessel function and j_{mn} is the n-th zero of J'_m :

$$J'_m(j_{mn}) = 0 \quad (10)$$

The axial wave number $k_{x,(m,n)}$ respect the dispersion equation:

$$k_{x,(m,n)} = k_0 \frac{M \pm \sqrt{1 - (1 - M^2)(\frac{j_{mn}}{kR})^2}}{1 - M^2} \quad (11)$$

Mode will propagate if:

$$kR \geq j_{mn}\sqrt{1 - M^2} \quad (12)$$

The radial wave number is:

$$k_{r,(m,n)} = \frac{j_{mn}}{R} \quad (13)$$

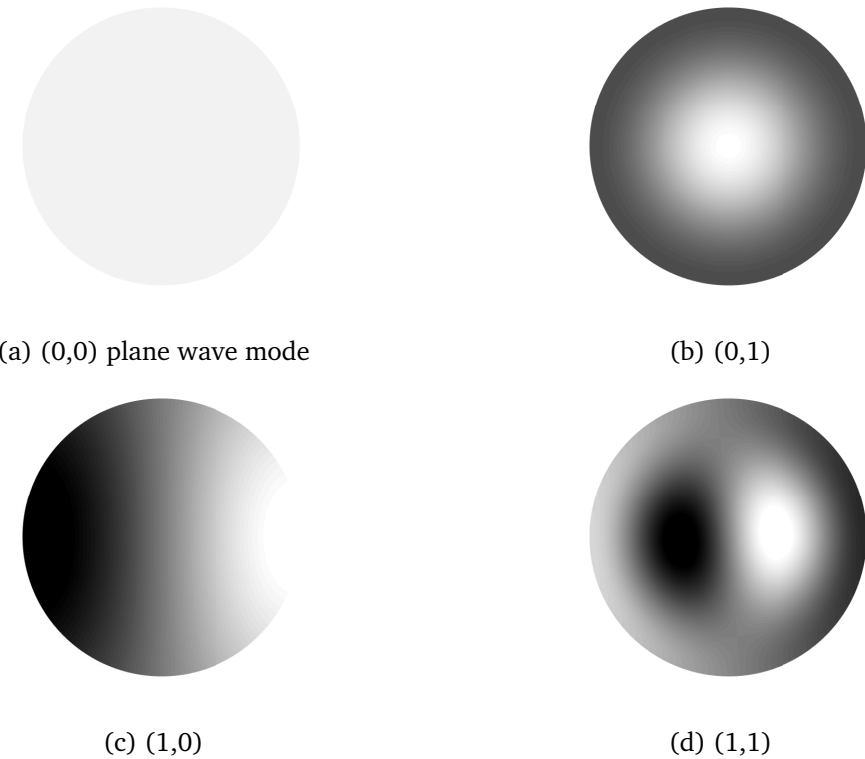


Figure 4: Mode shape in a circular duct

2.1.3 Wall attenuation

Model of attenuation

The viscosity is not negligible at the interface wall/flow. A model of attenuation given by Pierce [5] is:

$$k = \frac{\omega}{c} + (1+i) \frac{1}{2\sqrt{2}} \sqrt{\frac{\omega\mu}{\rho c^2}} \left[1 + \frac{\gamma-1}{\sqrt{Pr}} \right] \frac{L_p}{A} \quad (14)$$

Pr is the Prandtl number, ρ the density, L_p the perimeter and A the area. An easy way to use attenuation is to replace $k_0 = k$

Boundary condition: Ingard-Myers

For a wall of impedance Z , the boundary condition is still in discussion. Ingard assumes the continuity of acoustic particle displacement with uniform flow [6]. Myers extend the model for non-uniform mean-flow [7]:

$$\frac{\partial p}{\partial z}|_{wall} = \frac{ik}{Z} (1 - iM \frac{\partial}{\partial x})^2 p|_{wall} \quad (15)$$

2.2 Scattering matrix

The scattering matrix is a very powerful tool in the duct acoustic field. The applications are very different and the scattering matrix is also available for N-ports. To assess the acoustic properties of a liner, a lined section is placed between two hard duct wall:

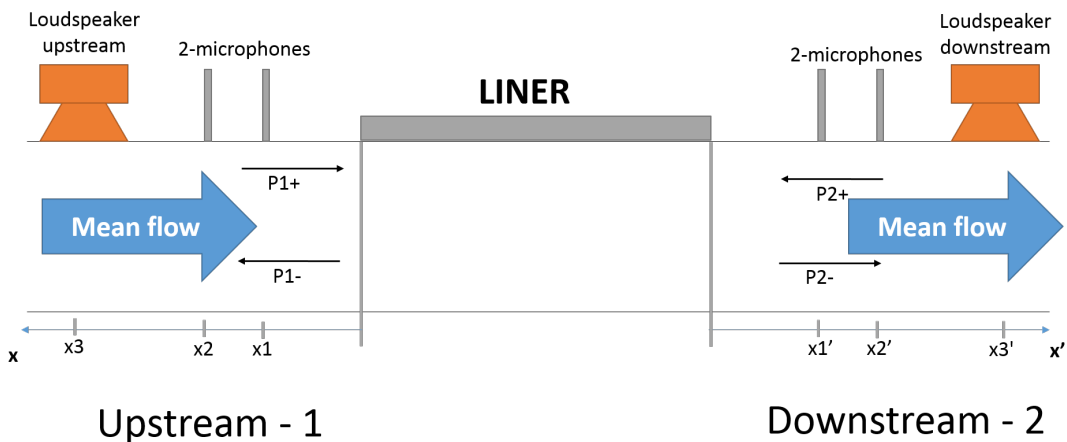


Figure 5: Scattering matrix setup

The excitation is one time at the upstream and one other time at the downstream. The properties are not equals for the downstream and the upstream because of the presence of a flow. The usual notation is p^+ for the wave which moves towards the lined section and p^- for the waves which moves off. The reflection and transmission coefficients are determined:

$$p^- = S p^+ \quad (16)$$

$$S = \begin{pmatrix} R_{11} & T_{21} \\ T_{12} & R_{22} \end{pmatrix} \quad (17)$$

$$\begin{pmatrix} p_1^- \\ p_2^- \end{pmatrix} = \begin{pmatrix} R_{11} & T_{21} \\ T_{12} & R_{22} \end{pmatrix} \begin{pmatrix} p_1^+ \\ p_2^+ \end{pmatrix} \quad (18)$$

However the pressures p_+ and p_- have to be preliminary determined. The well-known method of two-microphones is an easy way to do the wave decomposition [8]. For each measurement and for each side, two microphones measure the pressure p_1 and p_2 . The following system gives the pressures p_+ and p_- for the upstream or downstream case.

$$\begin{pmatrix} e^{ik_x^- x_1} & e^{-ik_x^+ x_1} \\ e^{ik_x^- x_2} & e^{-ik_x^+ x_2} \end{pmatrix} \begin{pmatrix} p^- \\ p^+ \end{pmatrix} = \begin{pmatrix} p_1 \\ p_2 \end{pmatrix} \quad (19)$$

It's possible to use more than 2 microphones, the system is over-determined.

$$\begin{pmatrix} e^{ik_x^- x_1} & e^{-ik_x^+ x_1} \\ \vdots & \vdots \\ e^{ik_x^- x_i} & e^{-ik_x^+ x_i} \\ \vdots & \vdots \\ e^{ik_x^- x_n} & e^{-ik_x^+ x_n} \end{pmatrix} \begin{pmatrix} p^- \\ p^+ \end{pmatrix} = \begin{pmatrix} p_1 \\ \vdots \\ p_i \\ \vdots \\ p_n \end{pmatrix} \quad (20)$$

There is lot of discussion about the combination of microphones which has to be used to get the more accurate decomposition.

To simplify the notations, since the beginning the pressure p was the complex pressure \hat{p} :

$$\hat{p}(\omega) = P(\omega)e^{i\phi(\omega)} \quad (21)$$

Where P is the amplitude and ϕ the phase (the reference is the source).

There are different methods to get this complex pressure. We used the Hilbert transform:

$$\tilde{x}(t) = x(t) + i \text{ Hilbert}[x(t)] = X(t)e^{i\psi(t)} \quad (22)$$

Where $\psi(t)$ is the instantaneous phase and $X(t)$ the temporal envelop of the signal. The instantaneous pulsation is:

$$\omega = \frac{d\psi}{dt} \quad (23)$$

For τ multiple of half of the excitation frequency, the true transfer function between the source and the microphone is:

$$H = \frac{2}{\tau} \int_0^\tau \frac{y(t)}{\tilde{r}(t)} dt \quad (24)$$

2.3 Impedance acoustic

There are several methods to determine the acoustic impedance. In this master thesis the single mode straightforward method and the mode matching method are implemented.

2.3.1 Impedance tube measurement

The older way to measure the impedance is the impedance tube measurement. A loud-speaker and the liner are mounted on the pipe extremities.

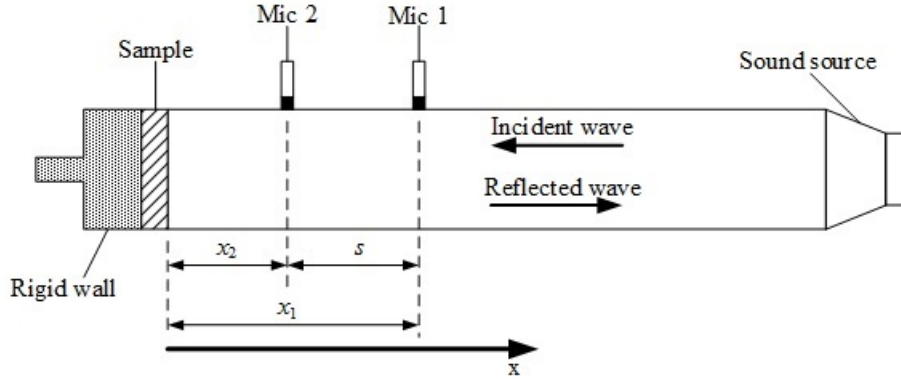


Figure 6: Impedance tube

The acoustic field is composed by stationary waves. The distance between two successive nodes can be measured and gives the impedance. This measure is not accurate. A more accurate measurement can be obtained thanks to a wave decomposition with the 2-microphones method. p^+ and p^- are determine and the impedance is given by [9]:

$$Z(w) = \rho c S \left[\frac{p^+ + p^-}{p^+ - p^-} \right] \quad (25)$$

2.3.2 The in-situ method

It is assumed that there is only the plane wave mode inside the cavity. The methods is describes in this paper [10]. One microphone measure the pressure field p_s flush with the liner surface. A second one is inside the cavity (height h) and measures p_c . The transfer function between the two microphones gives the impedance:

$$Z(w) = -i \frac{H_{cs}}{\sin(kh)} \quad (26)$$

The acoustic field measured is the close one. It's possible to move the first microphone to reduce the impact of the closed field:

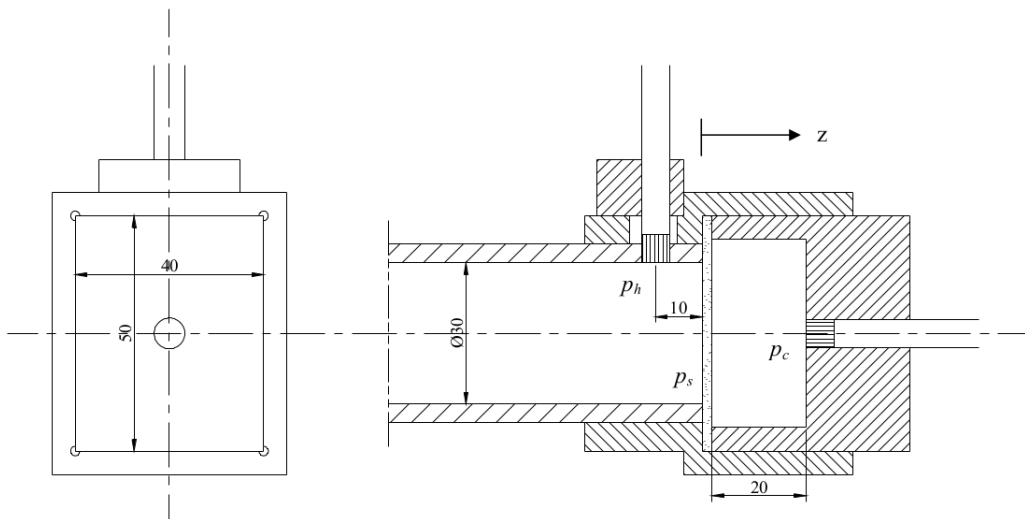


Figure 7: The in-situ method

2.3.3 The mode matching method

The mode matching method is a well-known method. The modes shapes have to be determined before. Each steps of the determination of these modes is in Appendix A: Modes for rectangular duct. The geometry is:

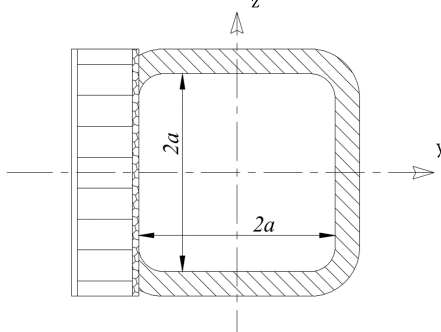


Figure 8: Rectangular duct lined for $y=-a$

Note that the coordinates are different from 2.1.1 Rectangular duct.

The incident wave is a plan wave, the direction y and z are independent. For the z direction, the boundary conditions are hard walls, the solutions are orthogonal. Thus there is just the $n = 0$ mode in the z direction. For the y direction the modes of the lined wall are not orthogonal, higher mode m will appear. The problem is reduced to a 2 dimensions probelm (x, y). The rig is decomposed in three parts:

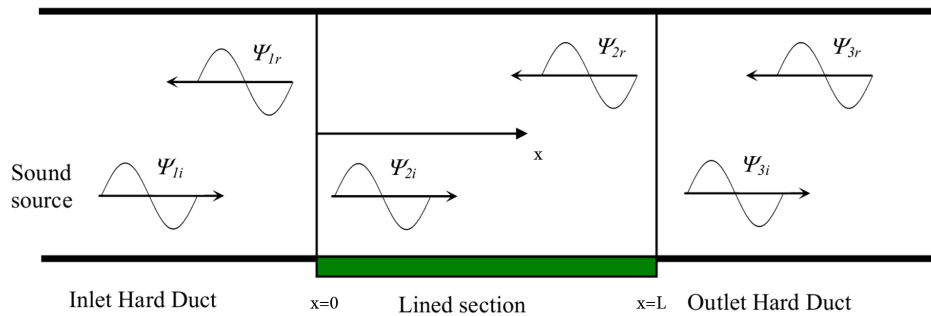


Figure 9: Coordinates for mode-matching

The pressures are given by:

- for the upstream hard section:

$$p_1(x, y) = a_1^+ \Psi_{1i,1}(y) e^{-ik_{x1i,1}x} + \sum_{m=0}^{\infty} a_m^- \Psi_{1r,m}(y) e^{ik_{x1r,m}x} \quad (27)$$

With $\Psi_{1i,m}(y) = \Psi_{1r,m}(y)$:

$$\begin{cases} \Psi_{1,m}(y) = 2 \cos\left(\frac{m\pi}{2a}y\right) & \text{for } n = 2p \\ \Psi_{1,m}(y) = 2i \sin\left(\frac{m\pi}{2a}y\right) & \text{for } n = 2p + 1 \end{cases} \quad (28)$$

- for lined section (one wall lined at the opposite of a hard wall):

$$p_2(x, y) = \sum_{m=0}^{\infty} b_m^+ \Psi_{2i,m}(y) e^{-ik_{x2i,m}x} + \sum_{m=0}^{\infty} b_m^- \Psi_{2r,m}(y) e^{ik_{x2r,m}(x-L)} \quad (29)$$

With:

$$\Psi_{2i,m}(y) = e^{ik_{y2i,m}y} - e^{-ik_{y2i,m}(y-2a)} \quad (30)$$

- for the downstream hard section:

$$p_3(x, y) = \sum_{m=0}^{\infty} c_m^+ \Psi_{3i,m}(y) e^{-ik_{x3i,m}(x-L)} + c_1^- \Psi_{3r,1}(y) e^{ik_{x3r,1}(x-L)} \quad (31)$$

With $\Psi_{3i,m}(y) = \Psi_{3r,m}(y)$:

$$\begin{cases} \Psi_{3,m}(y) = 2 \cos(\frac{m\pi}{2a}y) & \text{for } m = 2p \\ \Psi_{3,m}(y) = 2i \sin(\frac{m\pi}{2a}y) & \text{for } m = 2p + 1 \end{cases} \quad (32)$$

For the following part, the Mach number is considered zero to simplify the equation. Mode-matching with mean flow can be found here [11]. At each interface the pressure and the velocity are continuous:

$$p_1(0, y) = p_2(0, y) \quad (33)$$

and

$$p_2(L, y) = p_3(L, y) \quad (34)$$

$$\left. \frac{\partial p_1}{\partial x} \right|_{x=0} = \left. \frac{\partial p_2}{\partial x} \right|_{x=0} \quad (35)$$

and

$$\left. \frac{\partial p_2}{\partial x} \right|_{x=L} = \left. \frac{\partial p_3}{\partial x} \right|_{x=L} \quad (36)$$

By now the notation $k_{...,m} = k_{...}^{(m)}$ is used. Multiplied by $\Psi_1^{(u)}$ where $u=0..M$, and integrated over the cross-section:

$$\sum_{m=0}^{M-1} a_m^- \Lambda_{11}^{mu} - \sum_{m=0}^{M-1} b_m^+ \Lambda_{2i1}^{mu} - \sum_{m=0}^{M-1} b_m^- \Lambda_{2r1}^{mu} e^{-ik_{x2r}^{(m)}L} = -a_1^+ \Lambda_{11}^{1u} \quad (37)$$

$$\sum_{m=0}^{M-1} c_m^+ \Lambda_{11}^{mu} [1 + R_e] - \sum_{m=0}^{M-1} b_m^+ \Lambda_{2i1}^{mu} e^{-ik_{x2i}^{(m)}L} - \sum_{m=0}^{M-1} b_m^- \Lambda_{2r1}^{mu} = 0 \quad (38)$$

$$- \sum_{m=0}^{M-1} a_m^- \Lambda_{11}^{mu} k_{x1r}^{(m)} - \sum_{m=0}^{M-1} b_m^+ \Lambda_{2i1}^{mu} k_{x2i}^{(m)} + \sum_{m=0}^{M-1} b_m^- \Lambda_{2r1}^{mu} k_{x2r}^{(m)} e^{-ik_{x2r(m)}L} = -a_1^+ \Lambda_{11}^{1u} k_{x1i}^{(1)} \quad (39)$$

$$\sum_{m=0}^{M-1} c_m^+ \Lambda_{11}^{mu} (k_{x3i}^{(m)} - R_e k_{x3r(m)}) - \sum_{m=0}^{M-1} b_m^+ \Lambda_{2i1}^{mu} k_{x2i}^{(m)} e^{-ik_{x2i}^{(m)}L} + \sum_{m=0}^{M-1} b_m^- \Lambda_{2r1}^{mu} k_{x2r}^{(m)} e^{-ik_{x2r}^{(m)}L} = 0 \quad (40)$$

With R_e the reflection coefficient at the end of the duct and the index:

$$\Lambda_{pv}^{mu} = \iint_S \Psi_p^{(m)} \Psi_v^{(u)} ds \quad (41)$$

The true relations are for $M = \infty$. However the Index showed that the amplitudes of the higher modes quickly decrease. To avoid too much computation time, only the first modes are computed.

The system can be reduce to the following matrix:

$$\begin{bmatrix} \Lambda_{11}^{mu} & 0 & -\Lambda_{2i1}^{mu} & -\Lambda_{2ri1}^{mu} e^{-ik_{x2r}^{(m)} L} \\ 0 & \Lambda_{11}^{mu}[1 + R_e] & -\Lambda_{2i1}^{mu} e^{-ik_{x2i}^{(m)} L} & -\Lambda_{2r1}^{mu} \\ -\Lambda_{11}^{mu} k_{x1r}^{(m)} & 0 & -\Lambda_{2i1}^{mu} k_{x2i}^{(m)} & -\Lambda_{2ri1}^{mu} k_{x2r}^{(m)} e^{-ik_{x2r}^{(m)} L} \\ 0 & \Lambda_{11}^{mu}[k_{x3i}^{(m)} - R_e k_{x3r}^{(m)}] & -\Lambda_{2i1}^{mu} k_{x2i}^{(m)} e^{-ik_{x2i}^{(m)} L} & \Lambda_{2ri1}^{mu} k_{x2r}^{(m)} \end{bmatrix} \begin{bmatrix} a_m^- \\ c_m^+ \\ b_m^+ \\ b_m^- \end{bmatrix} \quad (42)$$

$$= \begin{bmatrix} -a_1^+ \Lambda_{11}^{1u} \\ 0 \\ -a_1^+ \Lambda_{11}^{1u} k_{x1i}^{(1)} \\ 0 \end{bmatrix} \quad (43)$$

With Λ_{pv}^{mu} a $M * M$ matrix. The index can be analytically calculated [11].

The system has $4M$ unknowns. To solve it, a_1^+ and R_e have to be measured. The two-microphones methods can be used in the upstream and downstream section.

2.3.4 The single mode straightforward method

This method is a simplified problem of the mode matching technique. For the the single mode straightforward method, it assumes that only the first mode exist in the lined section [2]. The amplitudes of the higher modes are considered negligible (for low frequency). Moreover if it assumes that there is just an incident wave ($b_{(1)}^- = 0$ and $c_{(1)}^- = 0$). With these assumptions:

$$k_{x2i}^{(1)} = \frac{i \ln \left(\frac{\tau_{13}}{1+R_{11}} \right)}{L}, \quad k_{x2r}^{(1)} = \frac{i \ln \left(\frac{\tau_{31}}{1+R_{33}} \right)}{L} \quad (44)$$

The impedance is given by 82

2.4 Optimum Cremer impedance

The problems consists to attenuate a specific mode. The problem is asymmetric with a locally reacting impedance, the boundary conditions are the Ingard-Myers conditions. The general dispersion relationship for a circular and annular duct:

$$k_{x,(m,n)} = k_0 \frac{M \pm \sqrt{1 - (1 - M^2) \left(\frac{k_{r,(mn)}}{R} \right)^2}}{1 - M^2} \quad (45)$$

The axial wave number depends only on the radial wave number. And with an impedance wall, the radial wave numbers are wander into their quarter of the complex plane in a irregular way.

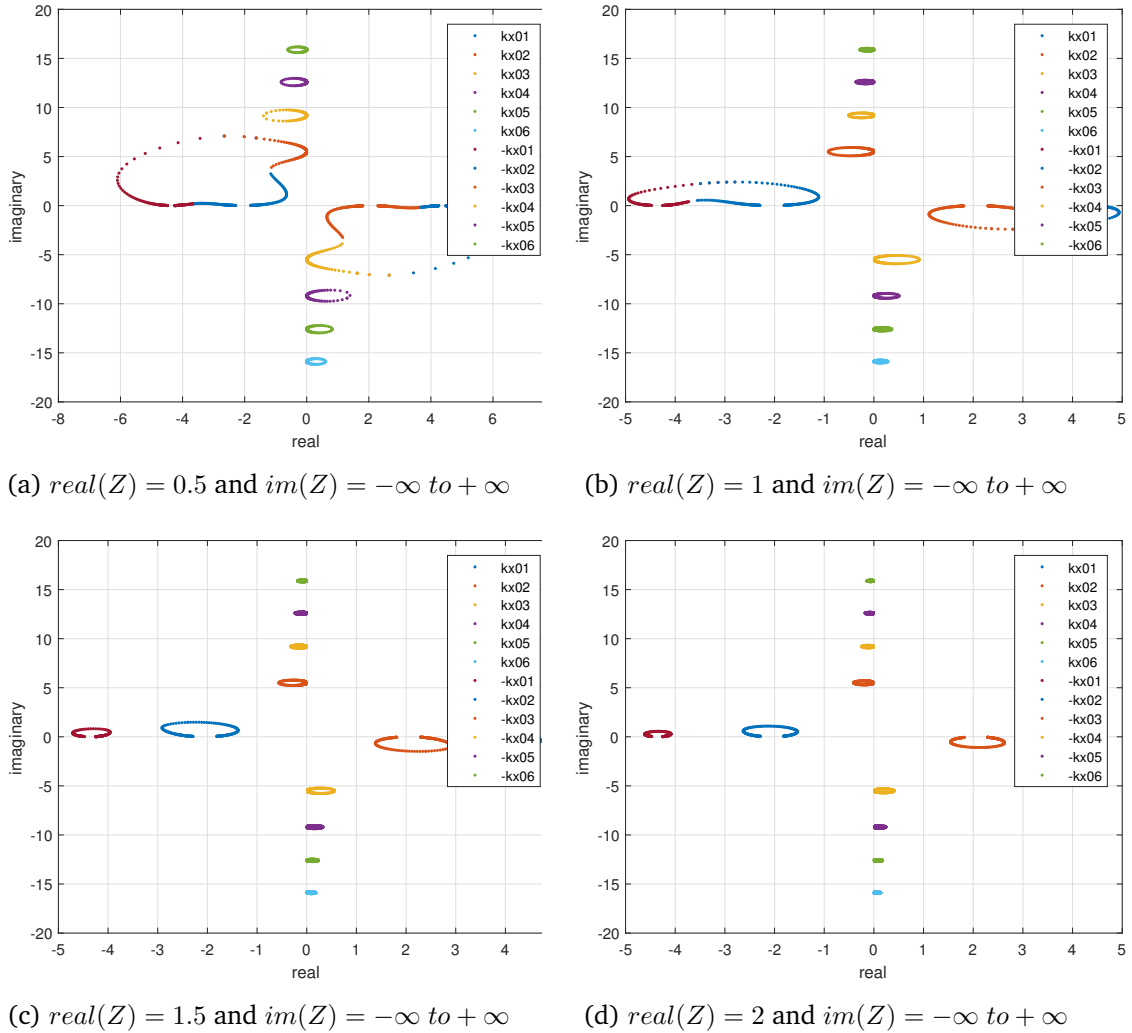


Figure 10: Axial wave numbers for $m = 0, kR = 4.353$ [12]

Cremer was the first to show the existence of a optimum radial wave number leading to the maximal axial decay rate of the least attenuate mode. This optimum condition correspond of the merging of two sequential order modes. For this specific condition the two modes collapse [13].

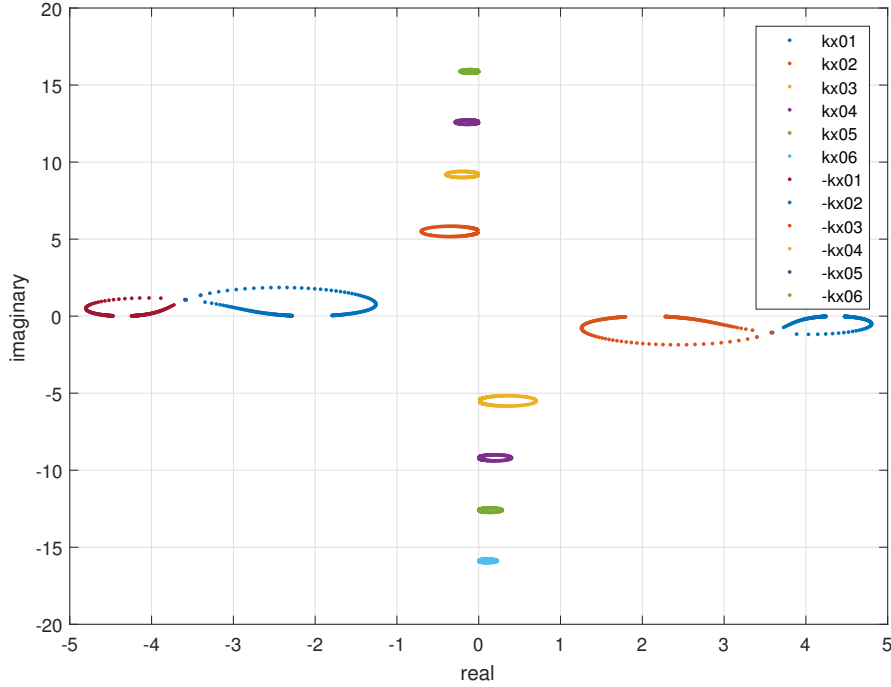


Figure 11: Axial wave number in the complex plan for $\text{Im}(Z)$ varying from $-\infty$ to $+\infty$ and for $\text{Re}(Z)=1.4165$. For $\text{Im}(Z)=-0.608$ the first two modes coalesce $k_{01} = k_{02} = 4.3 - 0.88i$ [13]

Cremer and Tester showed that this optimum wave number is given then the derived eigenvalue equation vanishes.

2.4.1 Optimization of a circular liner

The less attenuated mode has been found in an experimental setup and is the $(1, 0)$ mode. To simplify the notation $k_r = k_{r,(1,0)}$ is used. The assumption of high frequency is made [12]:

$$k_x \approx \frac{k}{1 \pm M_x} \quad (46)$$

The eigenvalue for the $(1, 0)$ mode is:

$$\frac{ikR}{Z} = (1 \pm M_x)^2 \frac{k_r r J'_1(k_r r)}{J_1(k_r r)} \quad (47)$$

The optimum radial wave number is:

$$\frac{d}{dk_r r} \left[(1 \pm M_x)^2 \frac{k_r r J'_1(k_r r)}{J_1(k_r r)} \right] = 0 \quad (48)$$

The equation is solved with the Matlab function "vpssolve". The optimum impedance determined is:

$$Z = 0.8918 - 0.3068i \quad (49)$$

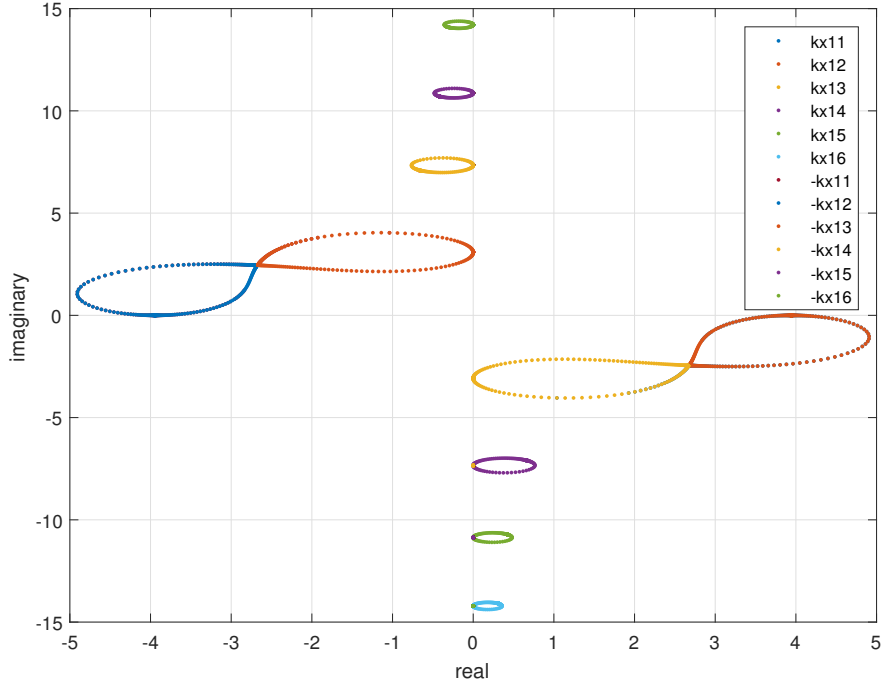


Figure 12: Axial wave number in the complex plan for $\text{Im}(Z)$ varying from $-\infty$ to $+\infty$ and for $\text{Re}(Z)=0.892$. For $\text{Im}(Z)=-0.307i$ the two modes coalesce $k_{11} = k_{12} = 4.4663 + 1.467i$ [13]

2.4.2 Optimization of an annular liner

The optimization of an annular liner is more difficult and is rarely done by an analytically method. On the contrary with the circular duct, the eigenvalue solutions are not simple. The second problem is that the less attenuate mode is rarely the plane wave mode. For our case, the less attenuate mode was the $(8, 0)$ and was determined by an experimental work. We tried to implement the Cremer impedance to reduce this mode. The general solution of the pressure field for annular ducts is:

$$p_{(m,n)} = \left[A_{mn} J_m(k_{r,(m,n)} r) + B_{mn} Y_m(k_{r,(m,n)} r) \right] \cos(m\theta) e^{i(\omega t - k_{x,(m,n)} x)} \quad (50)$$

Where J the Bessel function of the first type and order m and Y the Bessel function of the second type and order m .

From the general pressure solution and the Myers boundary conditions Eq.(15):

$$ik\beta_1 \left[1 - \left(\frac{k_{x,(m,n)}}{k} \right) M \right]^2 = k_{r,(m,n)} \left[\frac{A_{mn} J'_m(k_{r,(m,n)} b) + B_{mn} Y'_m(k_{r,(m,n)} b)}{A_{mn} J_m(k_{r,(m,n)} b) + B_{mn} Y_m(k_{r,(m,n)} b)} \right] \quad (51)$$

$$ik\beta_0 \left[1 - \left(\frac{k_{x,(m,n)}}{k} \right) M \right]^2 = k_{r,(m,n)} \left[\frac{A_{mn} J'_m(k_{r,(m,n)} a) + B_{mn} Y'_m(k_{r,(m,n)} a)}{A_{mn} J_m(k_{r,(m,n)} a) + B_{mn} Y_m(k_{r,(m,n)} a)} \right] \quad (52)$$

With β the admittance of the inner and external wall (radius b and a). For our application we choose to lined the external wall $\beta_1 = 0$ and the flow is zero $M = 0$.

The eigenvalue equation follows:

$$ika\beta_0 = -k_{r,(m,n)}a \left(\frac{J'_m(k_{r,(m,n)}a)Y'_m(k_{r,(m,n)}b) - J'_m(k_{r,(m,n)}b)Y'_m(k_{r,(m,n)}a)}{J_m(k_{r,(m,n)}a)Y'_m(k_{r,(m,n)}b) - J'_m(k_{r,(m,n)}b)Y_m(k_{r,(m,n)}a)} \right) \quad (53)$$

We solve $\frac{d}{d(k_r)}(Eq.(53)) = 0$ to find the optimum $k_{r,(m,n)}$. Then Eq.(53) is evaluated for this optimum wave number and gives the impedance.

The optimum impedance is:

$$Z = 0.4537 + 0.0148i \quad (54)$$

The eigenvalue equation has n solutions. To attenuate the modes (m, n) , the first m non zero solution has to be taken. The resolution is more detailed in Appendix B: Cremer optimum resolution with matlab.

3 Measurement and post-treatment

This part describes the experimental work from the setup to the calculation of the acoustic impedance. The post-treatment is also in this part. The theory is already described in 2 Theoretical acoustic.

3.1 Experimental work

3.1.1 KTH facilities

The Marcus Wallenberg Laboratory for Sound and Vibration has a flow test rig. The sketch of the facilities:

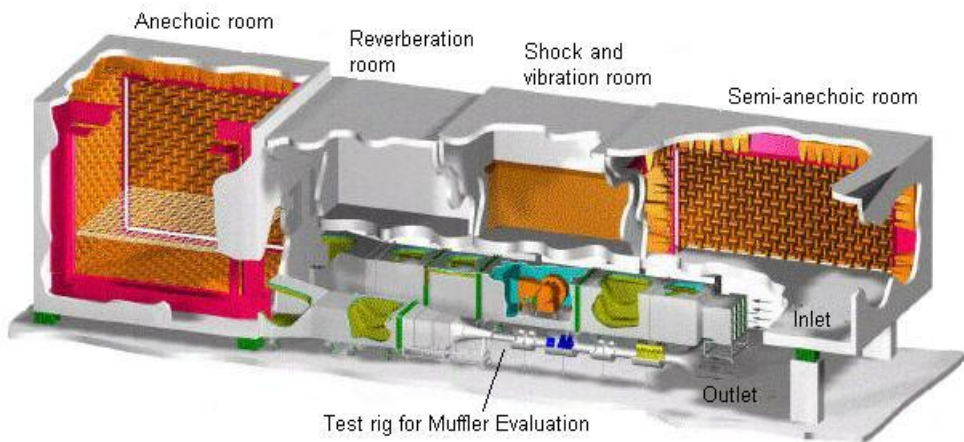


Figure 13: MWL flow acoustic test rig

The laboratory is equipped with a huge fan. For our experiments, this fan was linked to the anechoic room. The pressure increased and a flow was created in a rectangular rig. The anechoic room reduced the sound produced by the fan into the rig. This fan was controlled by a computer. During my master thesis, we had to fix the cooling system to be able to run the fan at 100% of its capacity.



Figure 14: Picture of the fan software

3.1.2 The rig setup

The setup is divided in three parts:

- Upstream numbered 1
- Lined section numbered 2
- Downstream numbered 3

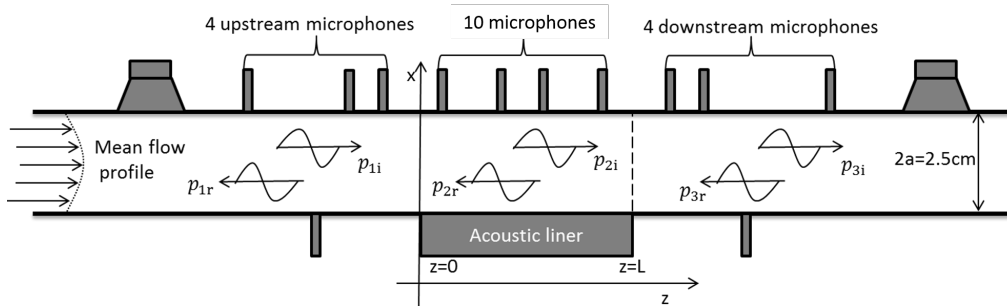


Figure 15: Sketch of liner test setup at KTH

2 loudspeakers and 16 microphones were used:

- 6 microphones to do the wave decomposition (3 at each upstream and downstream sides). Note than that 4 microphones were supposed to be used at the beginning.
- 10 microphones in the lined sections to measure the pressure field.

The termination of the rig was composed by a muffler. The reflection was very low but not equal to zero at the end of the rig.

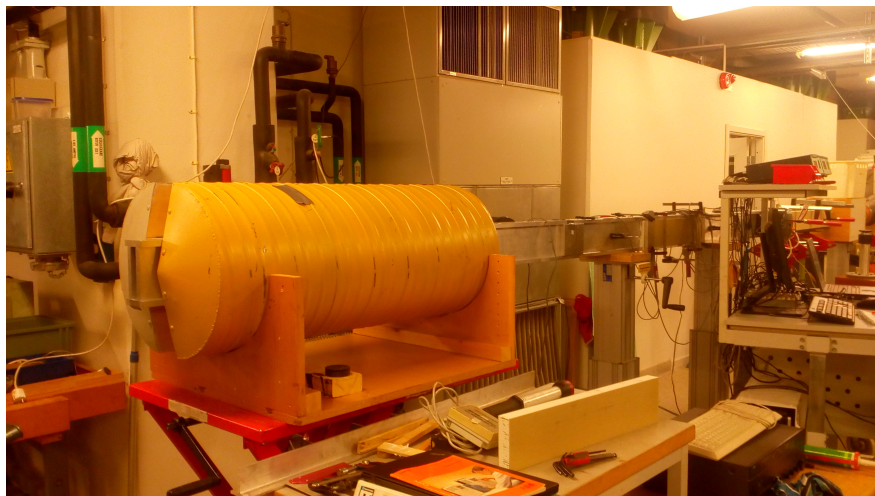


Figure 16: Picture of the Rig and the anechoic termination



Figure 17: Picture of the 16 microphones and the downstream loudspeaker

The liner was fixed flush with the wall. A small leakage could change the acoustic field.



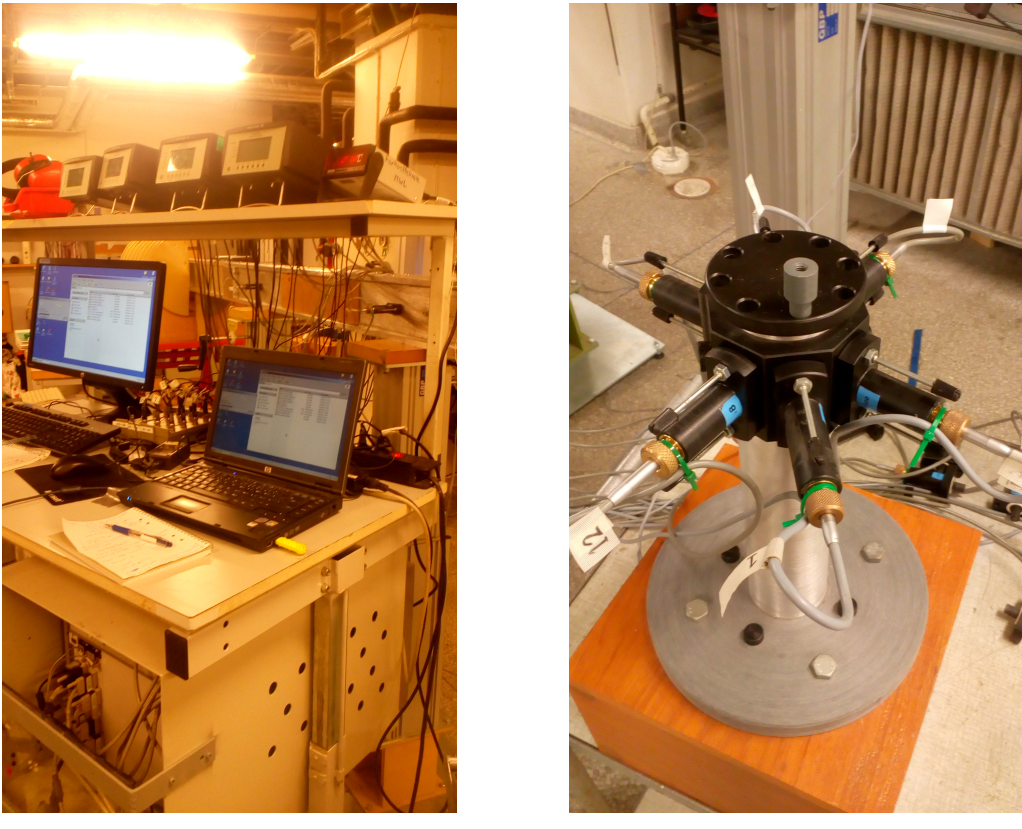
Figure 18: Picture of the acoustic liner fixed in the rig

The velocity of the flow had to be measured. The Appendix C: Mean flow measurement describes how to get the mean flow in the duct with the Pitot tube.



Figure 19: Picture of the Pitot tube

3.1.3 Acquisition chain



(a) Picture computer and nexuses

(b) Picture of the calibration tube

Figure 20: Pictures of experimental devices

A HP-VXI system creates an sinus excitation signal. This sinal is amplified by a classic amplifier and the loudspeaker transforms the signal into an acoustic sinus wave. The Brüel and Kjaer microphones provide an electric signal which is treat by a Nexus device. To get the true pressure value, the sensitivity and the gain of the nexus have to be saved. The HP-VXI system does also the acquisition. A Matlab program saves the temporal data into a file.

This code provided by Luck [4] has also other options to improve the quality of the measure:

- The excitation is calibrated before the measure to respect a positive plane wave p^+ equal to 1Pa . This calibration should avoid any non-linear pressure effect (this option is more important for high excitation levels)
- The time of the acquisition depends on the variance of the measured signals. The accuracy of the data increases with the measured time. But the temperature into the rig increases slowly during the measurement. The measure has to relatively fast to avoid any temperature effect.
- By the same idea, the frequencies studied are randomized. The effect of the temperature variation are distributed, and any temperature trend appears.

To get a more accurate measure, the microphones are calibrated before. A stationary wave is created in a tube. The axial position of the microphones are strictly the same as

are the measured pressures. The transfer functions is calculated, the reference is the first microphone.

3.1.4 Frequency domain and scattering matrix

The measures are time dependant:

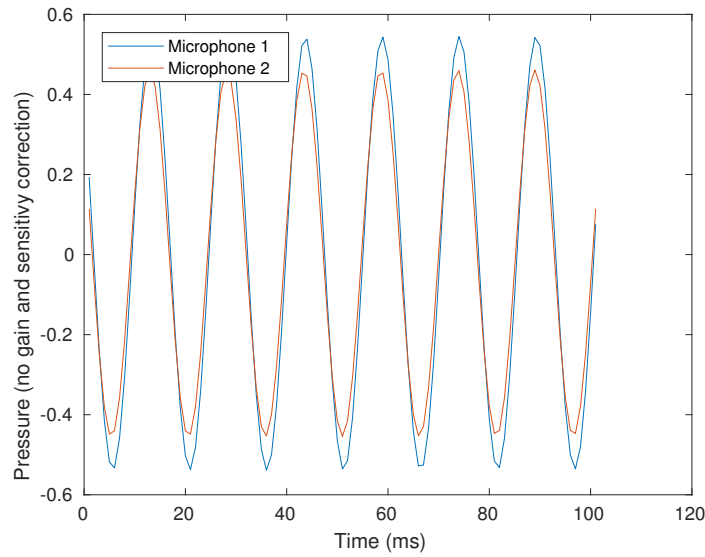


Figure 21: Time dependant signal

The Hilbert transform is used to get the estimated transfer function:

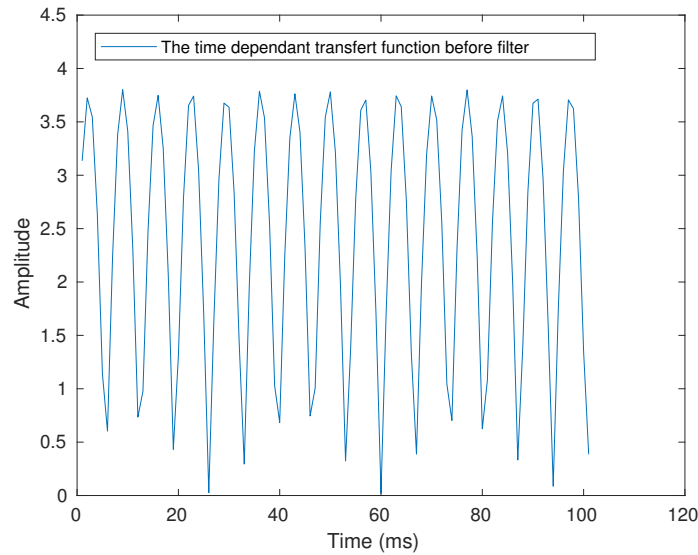


Figure 22: Estimated transfer function time dependant before window filtering

A window is determined which contained a whole number of sinus. The signal is filtered to get the true transfer function:

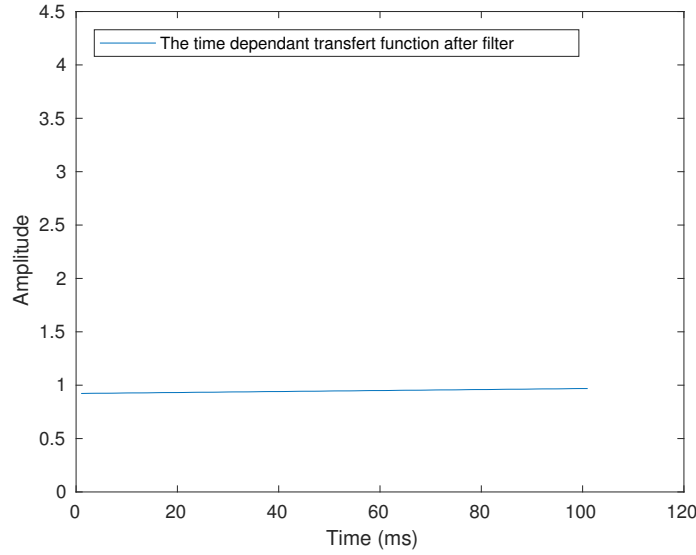


Figure 23: True transfer function time dependant after windows filtering

All the complex pressures are determined (relative to the source).

3.2 Reference: hard wall case

3 mach flows are studied: $M = 0$, $M = 0,08$ and $M = 0,16$. The frequency is between 700Hz and 1200Hz.

It's very difficult to get accurate measures in a rig. The mean flow adds lot of in-stationary noise. In a way to gain confidence in the results, a measure of the hard wall duct is performed. The problem is reduced to an infinite hard duct. Only a plane wave propagates because the higher modes are over the cut-off frequency. In this simple case the two transmission coefficients should be 1 and the reflection coefficients equal to zero.

The scattering matrix measured:

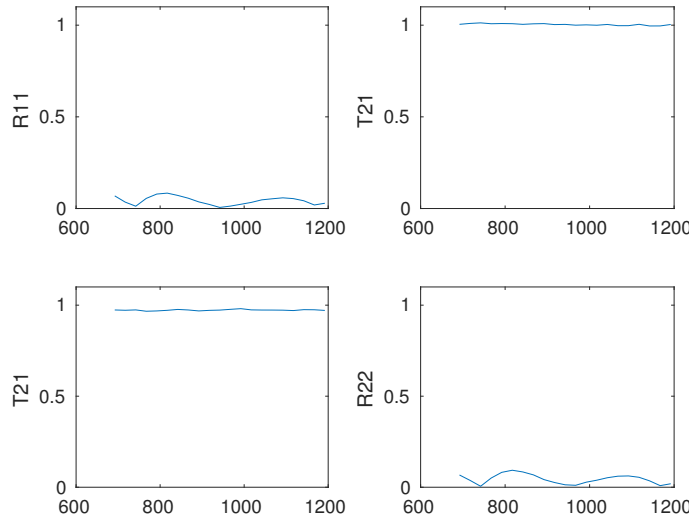


Figure 24: Scattering matrix: Hard wall and no flow

The transmission coefficients are very close to 1. The reflection is a little bit higher than expected. With flow, the scattering matrix stays very accurate:

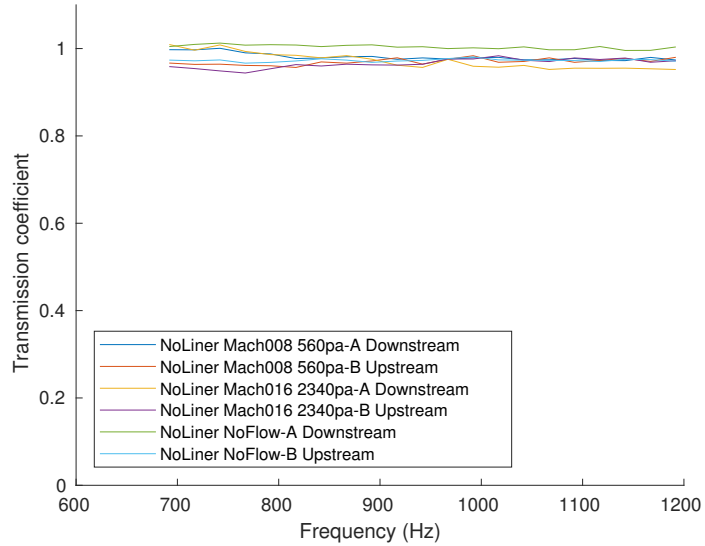


Figure 25: Transmission coefficients (T21 correspond to upstream and T12 correspond to downstream excitation): Hard wall; $M=0$, $M=0.08$, $M=0.16$

3.3 Acoustic liner

3.3.1 Scattering matrix and transmission loss

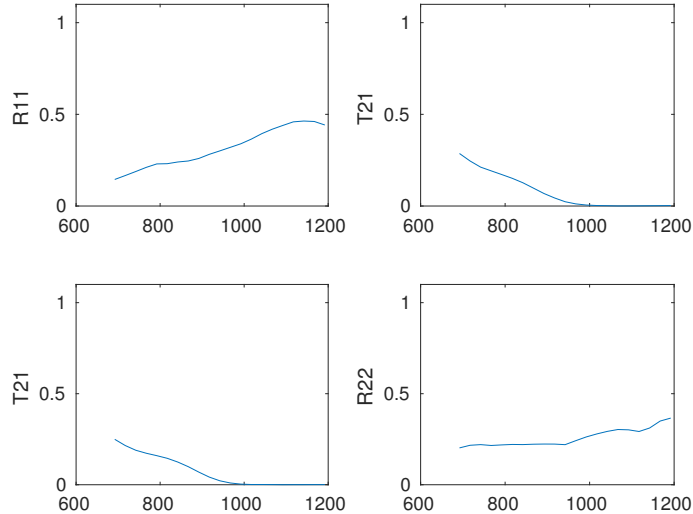


Figure 26: Scattering matrix: Liner and no flow

The reflection is lower than 0.5. Some energy is reflected towards the source. A liner has to reduce the acoustic energy transmit to the output. The transmission loss is

directly given by the transmission coefficient:

$$TL = 20\log(1/T) \quad (55)$$

Thus, the studied parameter is the transmission coefficient. As a reminder, upstream transmission coefficient is called T_{21} and the downstream T_{12} . For every case this coefficient is close to zero, almost all the acoustic energy is absorbed or reflected.

These coefficients are equal for no flow. The upstream coefficient becomes higher than the downstream coefficient with flow. This effect is due to the non uniform shape flow. At the wall the acoustic wave sees an opposite velocity gradient for the upstream or downstream propagation. This effect is not taken into account in the Myers boundary conditions which consider uniform flow. This difference is showed:

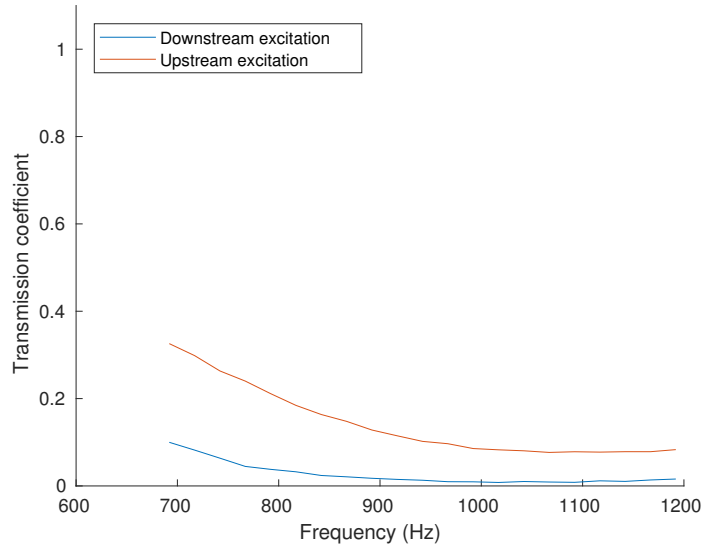


Figure 27: Transmission coefficients: Liner 1 and $M=016$

Two different effects of the flow are highlighted:

- Upstream excitation: the transmission increases with the mach number at low frequency
- downstream excitation: the efficiency of the liner increases at low frequency.

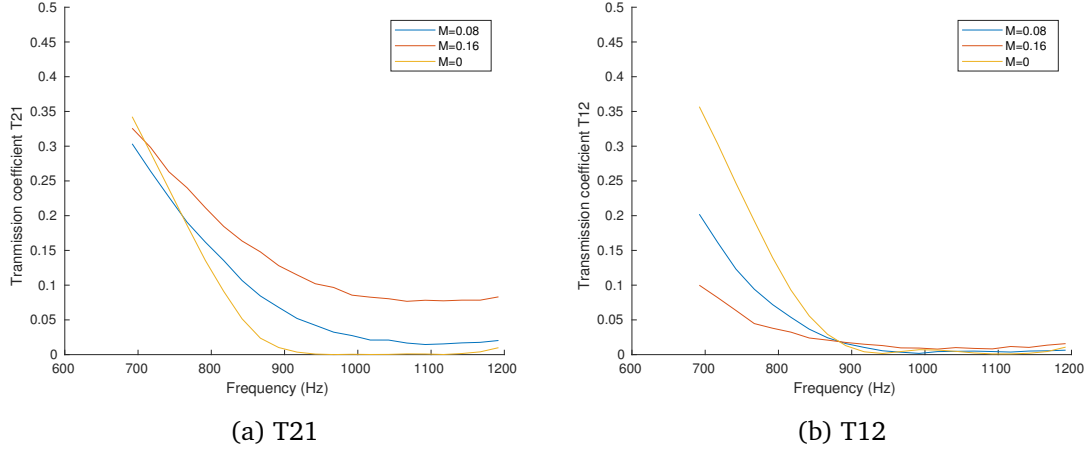


Figure 28: Transmission coefficients: Liner 1 and $M=0$, $M=0.08$, $M=0.16$

Liners should have the same dimensions and the same acoustic properties. However, no-negligible differences between these liners are highlighted:

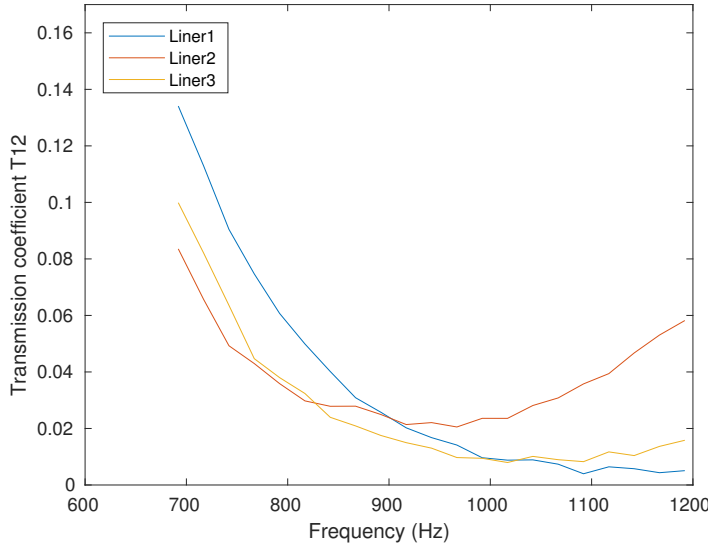


Figure 29: Transmission coefficients: liner 1, liner 2, liner 3 for $M=0.16$

The first results show the expected trends. The setup shows a good repeatability. Indeed two measures with the same liner were done (Two different fixations) and they are very closed.

The difference between the liners remains unexplained.

3.3.2 Acoustic impedance

A second step of post-treatment is to get the acoustic impedance.

4 Conclusion

Measures in a flow rig require theoretical knowledge. The specificity of the acoustical duct is the possibility to work with the modes because of the low amount of them.

Solving the convective Helmholtz equation allows to describe these modes and their shapes. In the axial direction a positive and a negative wave can propagate, the modes have different shapes in the section. For the rectangular duct, the different waves numbers are linked but the modes are independent in each direction. While for the annular case the circumferential and the radial modes are linked by a Bessel function. The optimization of an acoustic liner is not easy for two main reasons:

- The dimensions of the duct are very high compared to the dimensions of the liner cavities. The problem requires too many resources for numerical methods. The acoustic impedance has to be used to simplify the problem.
- The acoustic theory for lined wall in a circular duct is though. The optimum Tester and Cremer impedance is well determined to reduce the plane wave mode in a circular duct. In this master thesis, we tried to generalize it for a higher mode and for the annular case

To get the acoustic properties some tasks have to be done into the time data. This post-treatment is based on models and adds some uncertainties into the final values.

Last but not least the measurement with flow must be done carefully. The noise created by the flow is important.

The first results show a high transmission loss. However the disparity of the 3 liners seems to be high. The future determination of the impedance will confirm if something is wrong. There may be some manufactured defaults.

References

- [1] EEA (European Environment Agency). *Noise in Europe*. 2014.
- [2] L. Zhou. *Acoustic characterization of orifices and perforated liners with flow and high-level acoustic excitation*. 2015.
- [3] Rolls-Royce. *The jet engine*. 1992.
- [4] L. Peerlings. *Assessing precision and accuracy in acoustic scattering matrix measurements*. 2017.
- [5] D. Pierce. *Acoustics: an introduction to its physical principles and application*. 1994.
- [6] Ingard. *Influence of fluid motion past a plane boundary on sound reflection, absorption, and transmission*. 1959.
- [7] M.K. Myers. *On the acoustic boundary condition in the presence of flow*. 1980.
- [8] H. Bodén and M. Åbom. *Influence of errors on the two-microphone method for measuring acoustic properties in ducts*. 1984.
- [9] A. Russel. *Absorption Coefficients and Impedance*. 2015.
- [10] T. Elnady and H. Bodén. *An Inverse Analytical Method for Extracting Liner Impedance from Pressure Measurements*. 2008.
- [11] T. Elnady and H. Bodén. *Validation of an Inverse Semi-Analytical Technique to Educe Liner Impedance*. 2009.
- [12] R. Kabral. *Turbocharger aeroacoustics and optimal damping of sound*. 2017.
- [13] S. Rienstra and A. Hirschberg. *An Introduction to Acoustics*. 2016.

5 Appendix

Appendix A: Modes for rectangular duct

The duct geometry is:

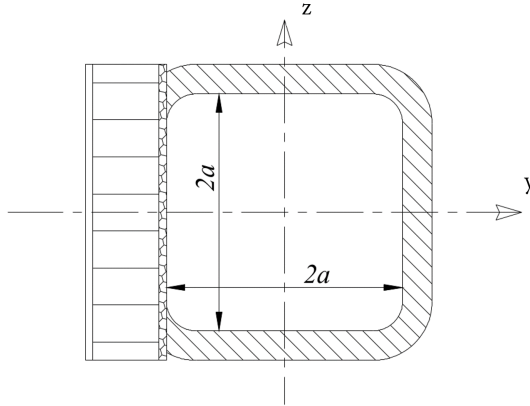


Figure 30: Rectangular duct lined for $y = -a$

The Convective Helmholtz equation in the Cartesian coordinates:

$$\Delta p + \left[(w - ku_0)^2 - k^2 c_0^2 \right] p = 0 \quad (56)$$

A resolution by separation of variables gives this decomposition:

$$p(x, y, z, \omega) = \sum_{l=0}^{\infty} p_l^+ \Psi_{(m,n)}(x, y, z) + p_l^- \Psi_{(m,n)}(x, y, z) \quad (57)$$

With:

$$\Psi_{(m,n)}(x, y, z) = (A_m e^{ik_{y,(m,n)}} + B_m e^{-ik_{y,(m,n)}})(A_n e^{ik_{z,(m,n)}} + B_n e^{-ik_{z,(m,n)}}) e^{-ik_{x,(M,\omega)}x} \quad (58)$$

Hard duct

Starting with the general form:

$$\Psi(x, y, z) = (A e^{ik_y y} + B e^{-ik_y l})(C e^{ik_z z} + D n e^{-ik_z z}) e^{-ik_x (M, \omega) x} \quad (59)$$

The boundary conditions in the z direction are the hard wall conditions, the velocity is zero:

$$\left. \frac{\partial \Psi}{\partial z} \right|_{z=\pm a} = 0 \quad (60)$$

Give the system:

$$\begin{cases} C e^{-ik_z a} - D e^{ik_z a} = 0 \\ C e^{ik_z a} - D e^{-ik_z a} = 0 \end{cases} \quad (61)$$

In the matrix form:

$$\begin{bmatrix} e^{-ik_z a} & -e^{ik_z a} \\ e^{ik_z a} & -e^{-ik_z a} \end{bmatrix} \begin{pmatrix} C \\ D \end{pmatrix} = \begin{pmatrix} 0 \\ 0 \end{pmatrix} \quad (62)$$

The eigenvalue equation:

$$-e^{-i2k_z a} + e^{i2k_z a} = 0 \iff \sin(2ka) = 0 \quad (63)$$

The wave number of order n :

$$k_{z,n} = \frac{n\pi}{2a}; n \in N \quad (64)$$

Compute in the system Eq.(61)

$$\begin{cases} C_n e^{-i\frac{n\pi}{2}} - D_n e^{i\frac{n\pi}{2}} = 0 \\ C_n e^{i\frac{n\pi}{2}} - D_n e^{-i\frac{n\pi}{2}} = 0 \end{cases} \quad (65)$$

Thus:

$$C_n(-i)^n - D_n(i)^n = 0 \quad (66)$$

Two cases $n = 2p$ or $n = 2p + 1$

$$C_n = D_n \text{ for } n = 2p \text{ and } C_n = -D_n \text{ for } n = 2p + 1 \quad (67)$$

Two solution for the mode shapes:

$$\Psi_n(z) = 2 \cos\left(\frac{n\pi}{2a}z\right) \text{ for } n = 2p \text{ and } \Psi_n(z) = 2i \sin\left(\frac{n\pi}{2a}z\right) \text{ for } n = 2p + 1 \quad (68)$$

Finally for two opposite hard walls the mode shapes are:

$$\begin{cases} \Psi_n(z) = 2 \cos\left(\frac{n\pi}{2a}z\right) \text{ for } n = 2p \\ \Psi_n(z) = 2i \sin\left(\frac{n\pi}{2a}z\right) \text{ for } n = 2p + 1 \end{cases} \quad (69)$$

Note that only the modes below the cut-off frequency propagate. The higher mode are quickly attenuated.

Lined walls

Starting with the general form:

$$\Psi(x, y, z) = (Ae^{ik_y y} + Be^{-ik_y, ly})(Ce^{ik_z z} + Dne^{-ik_z z})e^{-ik_x(M, \omega)x} \quad (70)$$

The boundary conditions in the y direction one lined wall and a hard wall, the velocity is respectively 0 and given by the Myers condition:

$$\frac{\partial \Psi}{\partial y} \Big|_{y=+a} = 0 \quad (71)$$

$$\frac{\partial p}{\partial y} \Big|_{y=-a} = \frac{ik}{Z} \left(1 - iM \frac{\partial}{\partial x}\right)^2 p \Big|_{y=-a} \quad (72)$$

Give the system:

$$\begin{cases} Ae^{ik_y a} - Be^{-ik_y a} = 0 \\ Aik_y e^{-ik_y a} - Bik_y e^{ik_y a} = ikA(1 - \frac{Mk_x}{k})^2 [Ae^{-ik_y a} - Be^{ik_y a}] \end{cases} \quad (73)$$

Using the wave dispersion equation:

$$k_x^2 + k_y^2 = (k - Mk_x)^2 \quad (74)$$

Using this relation in the Myers condition:

$$\begin{cases} Ae^{ik_y a} - Be^{-ik_y a} = 0 \\ Ak_y e^{-ik_y a} - Bk_y e^{ik_y a} = \frac{A}{k}(k_x^2 + k_y^2)[Ae^{-k_y a} - Be^{k_y a}] \end{cases} \quad (75)$$

The matrix form:

$$\begin{bmatrix} e^{ik_y a} & -e^{-ik_y a} \\ k_y e^{-ik_y a} - \frac{A}{k}(k_x^2 + k_y^2)[e^{-k_y a}] & -k_y e^{ik_y a} - \frac{A}{k}(k_x^2 + k_y^2)[-e^{k_y a}] \end{bmatrix} \begin{pmatrix} A \\ B \end{pmatrix} = \begin{pmatrix} 0 \\ 0 \end{pmatrix} \quad (76)$$

The eigenvalue equation:

$$-k_y(e^{i2k_y a} - e^{-i2k_y a}) - (e^{2ik_y a} + e^{-2ik_y a})(\frac{A}{k}(k_x^2 + k_y^2)) = 0 \quad (77)$$

The final eigenvalue equation:

$$k_y \tan(2k_y a) - i(\frac{A}{k}(k_x^2 + k_y^2)) = 0 \quad (78)$$

This equation has m solution, called modes. Thus the wave number $k_{y,m}$ is the $m - th$ k_r solution of the eigenvalue equation Eq.(78). The first line of the system Eq.(5) gives an other condition for the amplitudes:

$$A_m e^{ik_{y,m} a} - B_m e^{-ik_{y,m} a} = 0 \iff B_m = A_m e^{i2k_{y,m} a} \quad (79)$$

Finally for a lined wall opposite to a hard walls the mode shapes are:

$$\Psi_m(y) = e^{ik_{y,m} y} - e^{-ik_{y,m} (y-2a)} \text{ with } k_{y,m} \text{ solution of Eq.(78)} \quad (80)$$

Note than the relation:

$$\frac{\frac{\partial \Psi_l}{\partial y}|_{y=-a}}{p|_{y=-a}} = k_y \tan(2k_y a) \quad (81)$$

And compute in the Myers boundary conditions gives directly the impedance:

$$Z = \frac{i(k - Mk_x)^2}{k k_y \tan(2ak_y)} \quad (82)$$

Appendix B: Cremer optimum resolution with matlab

The circular resolution is very similar to the annular resolution. The least attenuated mode is the (m, n) and the radial wave number is $k_r = k_{r,(m,n)}$. A function $F(k_r)$ is defined as the derivative of the eigenvalue equation. The function "vpsole" solve $F = 0$ using a starting point called "initial guess".

To preliminary find the "initial guess point", $1/F(k_r)$ is plotted in the complex plan:

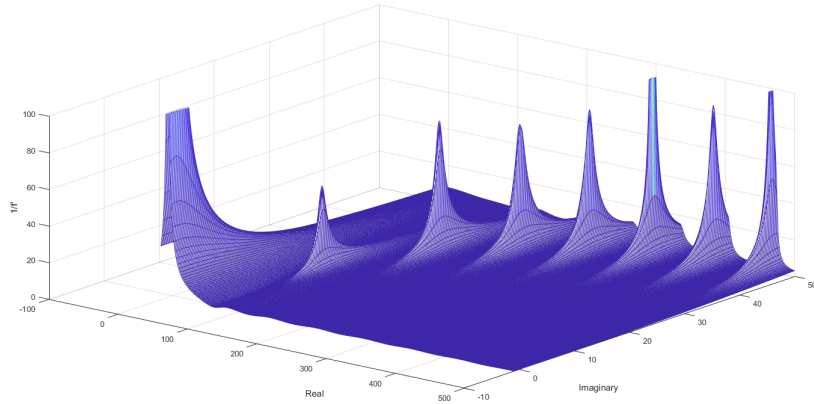


Figure 31: $1/F(k_r)$ in the complex plan

Every peak corresponds to a root of $F(k_r)$ and the approximate coordinates are used in the "vpsole" as initial guess.

The first n solutions are represented in the graph:

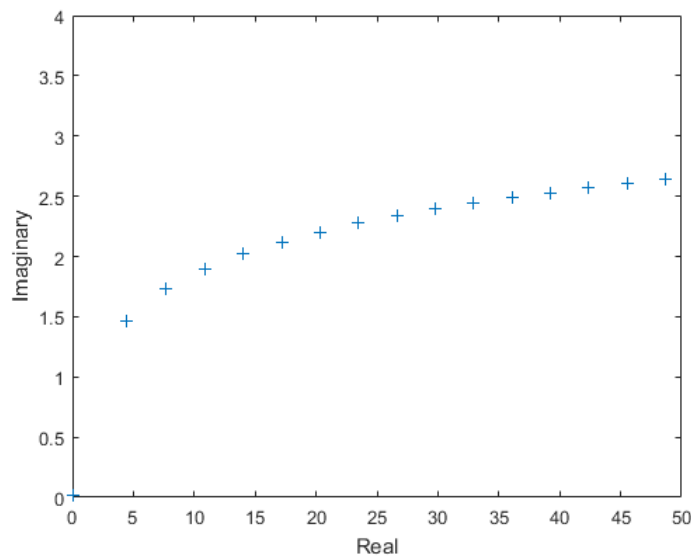


Figure 32: $k_{r,(1,n)}$ solution of $F = 0$ for the circular case

The n non zero is the optimum radial wave number $k_{r,(m,n)}$

Appendix C: Mean flow measurement

The Pitot tube measures the dynamic p_t pressure thanks to a manometer. The atmospheric pressure is called P_s . Two models exist:

- Incompressible fluid

$$u = \sqrt{\frac{2(p_t - p_s)}{\rho}} \quad (83)$$

- Compressible fluid

$$\frac{p_t}{p_s} = \left(1 + \frac{\gamma - 1}{2} M^2\right)^{\frac{\gamma}{\gamma-1}} \quad (84)$$

The two models are drawn in a graphic:

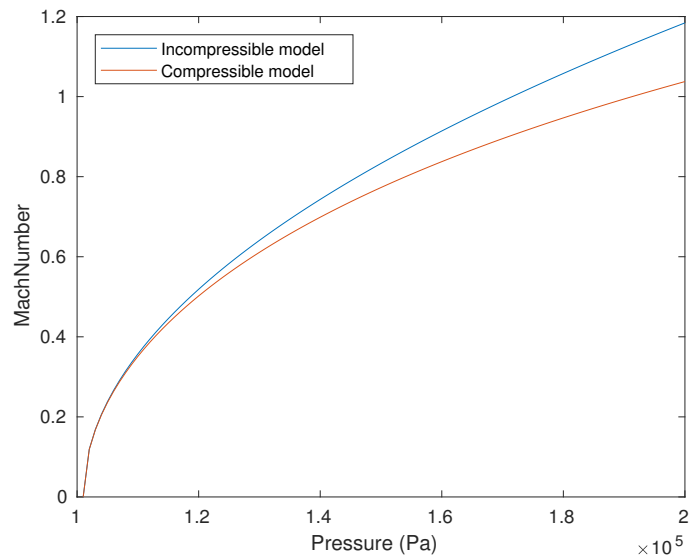


Figure 33: Two different models for Pitot tube

For mach number below 0.2 both models give approximately the same value. However, the pressure is measured in the middle of the section and get the maximal velocity. Indeed the profil of the velocity across the section is not uniform as showed the following graphic:

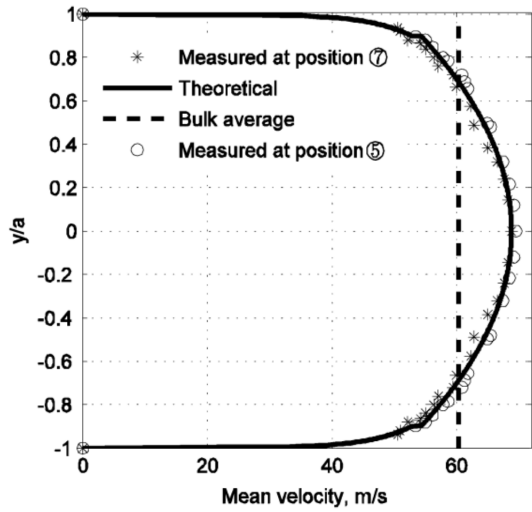


Figure 34: Flow profile across a section [2]

A correction coefficient between the mean mach number and the maximum mach number is applied. It was determined with a linear regression based on experimental values [2].

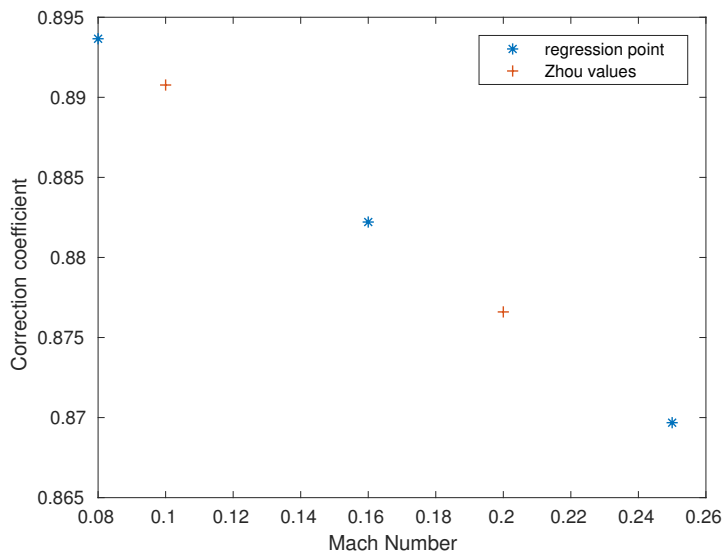


Figure 35: Linear regression

The target mach numbers used in this report were 0.08 and 0.16 and are the mean mach number value.